

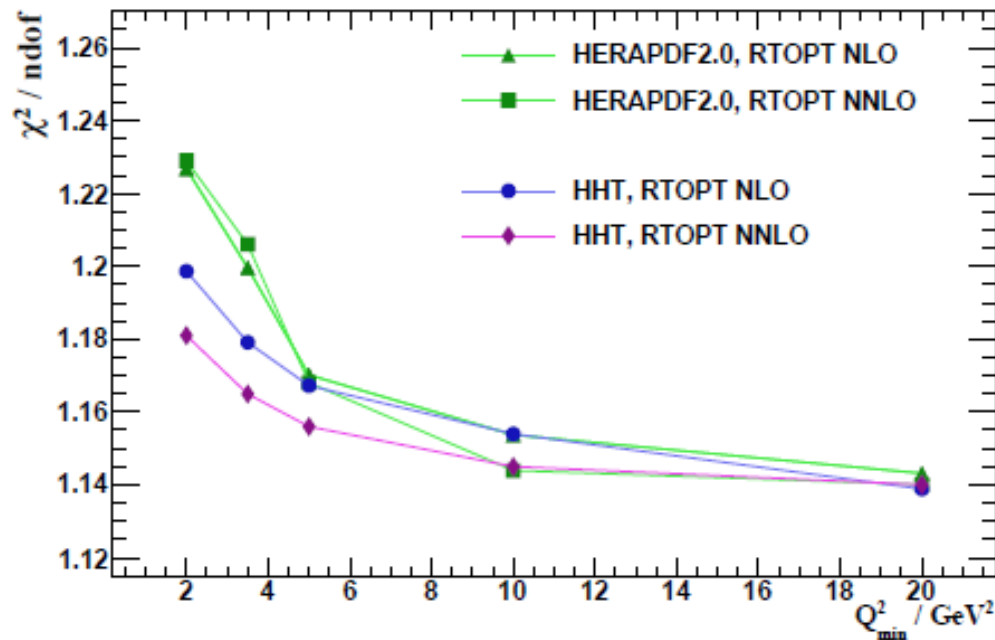
# Impact of low-x resummation on QCD analysis of HERA data

xFitter developer's team  
A M Cooper-Sarkar

## **Low-x resummation:**

- Improves the description of HERA data at low-x, low- $Q^2$ , high-y, *without need for further parameters (as for example when adding higher twist terms)*
- Results in a rising low-x gluon, which is always larger than the total Sea

The  $\chi^2/\text{ndof}$  of the HERAPDF2.0 NLO and NNLO fits deteriorate as the minimum value of  $Q^2$  for data entering the fit is lowered



One way to improve this is to add higher twist terms - HHT analysis 1604.02299

But low  $Q^2$  is also low  $x$  and we have long suspected that the low- $x$  region could require BFKL- $\ln(1/x)$  resummation. This does not require any extra parameters to fit the data (as higher twist does). It requires extending the DGLAP formalism to include  $\ln(1/x)$  resummation. The tool to do this is the HELL code (Bonvini et al)

# HELL has been implemented in xFitter

Here we explore consequences for a HERAPDF style fit

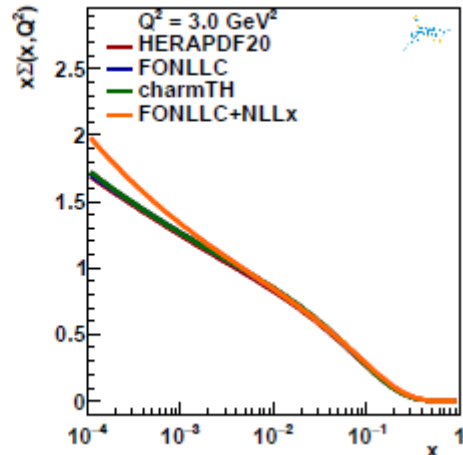
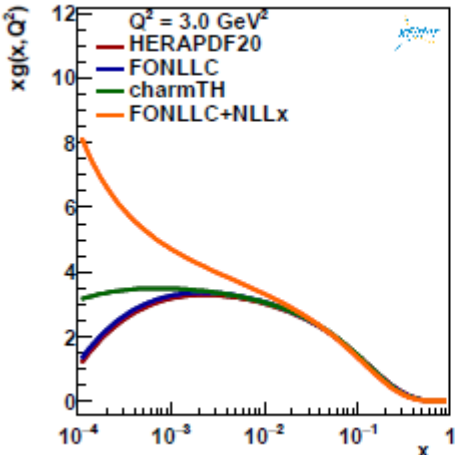
HELL implements resummation corrections to the fixed order splitting functions and coefficient functions up to NLL accuracy in  $\ln(1/x)$ , denoted as NLLx. The fixed order quantities are calculated by APFEL within the FONLL variable flavour number scheme. Thus we must use FONLL for the HERAPDF fit

The computation of  $\ln(1/x)$  resummation is unreliable at low scales due to the large value of  $\alpha_s$  thus the starting scale is raised to  $Q_0^2=2.56\text{GeV}^2$  rather than the usual HERAPDF value of  $Q_0^2=1.9\text{GeV}^2$ . Consequently the charm quark threshold,  $\mu_c$ , must be displaced above  $Q_0$  while keeping the charm mass,  $m_c$ , fixed. (see 1707.05343)

Finally NLLx resummation can be applied

HERAPDF2.0 NNLO	FONLL-C	Move $Q_0^2$ and charm threshold	include NLLx resummation
1363/1131	1387/1131	1389/1131	1316/1131

HERA  $\chi^2/\text{d.o.f}$



The  $\chi^2$  for the NNLO fit improves dramatically at this final step

The shape of the gluon is also changed dramatically from flattening/turning over at low-x to singular at low-x

## Technical aside

HERAPDF2.0 NNLO	FONLL-C	Move $Q_0^2$ and charm threshold	include NLLx resummation
1363/1131	1387/1131	1389/1131	1316/1131

The increase in  $\chi^2$  for FONLLC is due to the treatment of FL, for which terms up to  $d\bar{\sigma}(\alpha_S^3)$  are included for RTOPT, but terms up to  $di\bar{\sigma}(\alpha_S^2)$  are included for FONLLC

The slight change in shape of the gluon when the charm threshold is displaced is partly due to the PDF matching conditions. Moving up the charm threshold using fixed order NNLO depresses the charm PDF at larger scales. Since charm is generated by gluon splitting this requires a slightly larger gluon to compensate. However PDF matching conditions are also affected by logs of  $1/x$ , which are resummed in HELL such that the spread caused by matching is significantly reduced for NNLO+NLLx.

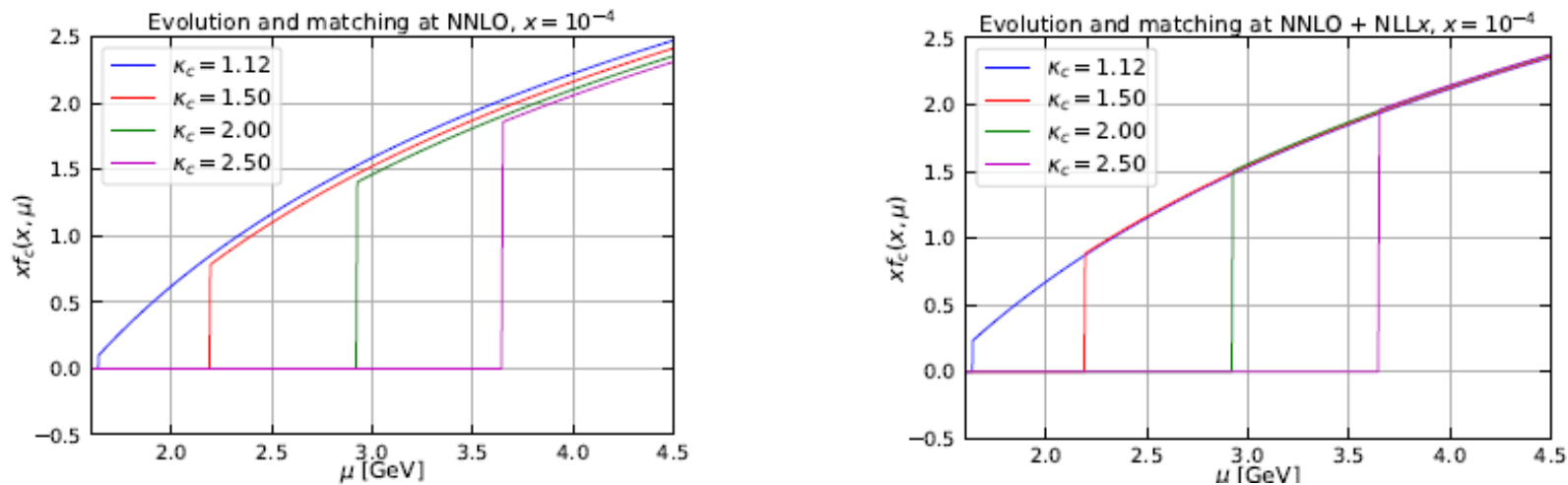


**Figure 1** The charm PDF at  $x = 10^{-4}$  as a function of the factorisation scale  $\mu$  for different values of the charm threshold  $\mu_c = \kappa_c m_c$ , with  $\kappa_c = 1.12, 1.5, 2, 2.5$ . The plots show the effect of the matching at NNLO (upper plot) and at NNLO+NLLx (lower plot).

## Further considerations:

Since we have change the heavy quark scheme the charm and beauty masses used may not be optimal for the new scheme. Thus charm and beauty data from HERA are included in the fit and [charm and beauty mass scans](#) are performed to determine new values  $m_c=1.46$  and  $m_b=4.5\text{GeV}$ . Only  $m_c$  differs from that of the HERAPDF and the charm threshold is move to  $\mu_c=1.64$  correspondingly. We retain charm data in the main fit since it is potentially sensitive to low  $x$  resummation.

Since we have a very different shape of the gluon PDF a [parametrisation scan](#) is performed at NNLO+NLLx to determine if the HERAPDF parametrisation is adequate. The form of the parametrisation is confirmed, however the negative term in the gluon is now small  $\sim 3\sigma$  from zero. In fact this is also the case for the NNLO fit due to the raised starting scale  $Q_0^2=2.56\text{GeV}^2$

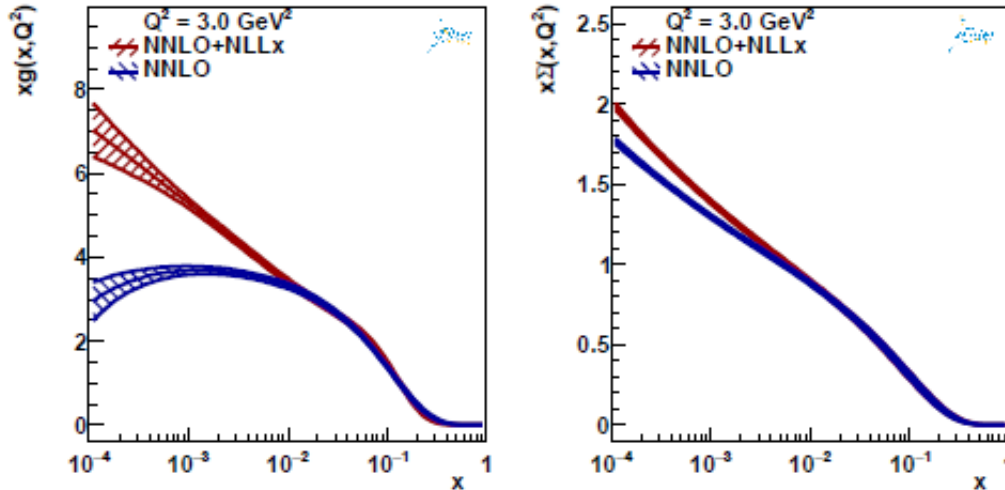
Nevertheless the resulting gluon shapes are very different.

The form of the common parametrisation used for both NNLO and NLLx is

$$\begin{aligned}xg(x) &= A_g x^{B_g} (1-x)^{C_g} - A'_g x^{B'_g} (1-x)^{C'_g}, \\xu_v(x) &= A_{u_v} x^{B_{u_v}} (1-x)^{C_{u_v}} (1 + E_{u_v} x^2), \\xd_v(x) &= A_{d_v} x^{B_{d_v}} (1-x)^{C_{d_v}}, \\x\bar{U}(x) &= A_{\bar{U}} x^{B_{\bar{U}}} (1-x)^{C_{\bar{U}}} (1 + D_{\bar{U}} x), \\x\bar{D}(x) &= A_{\bar{D}} x^{B_{\bar{D}}} (1-x)^{C_{\bar{D}}}.\end{aligned}$$

Note it is not the negative term which makes the gluon turn over at low- $x$  for NNLO, the main term can also have a valence like shape if  $B_g$  is positive.

After these adjustments – and adding experimental uncertainties we have



## A decrease in $\chi^2$ of 73

Largely due to the NC e+p 920 data

But also less need for shifts of systematic uncertainties

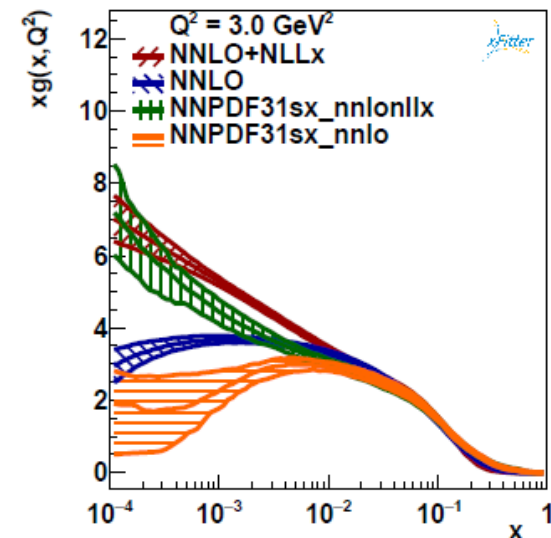
$$\chi^2 = \sum_i \frac{[D_i - T_i (1 - \sum_j \gamma_j^i b_j)]^2}{\delta_{i,unc}^2 T_i^2 + \delta_{i,stat}^2 D_i T_i} + \sum_j b_j^2$$

$$+ \sum_i \ln \frac{\delta_{i,unc}^2 T_i^2 + \delta_{i,stat}^2 D_i T_i}{\delta_{i,unc}^2 D_i^2 + \delta_{i,stat}^2 D_i^2},$$

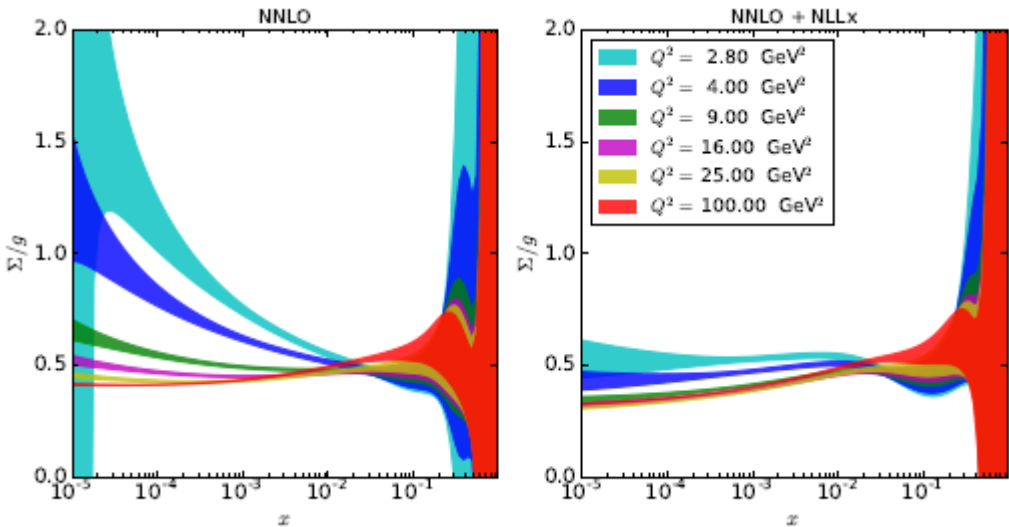
	NNLO fit with new settings	NNLO+NLLx fit with new settings
Total $\chi^2$ /d.o.f	1446/1178	1373/1178
subset NC 920 $\chi^2$ /n.d.p	446/377	413/377
subset NC 820 $\chi^2$ /n.d.p	70/70	65/70
subset charm $\chi^2$ /n.d.p	48/47	49/47
correlated shifts inclusive	102	77
correlated shifts charm	15	11
log term inclusive	20	-3
log term charm	-2	-1

NNPDF: arXiv:1710.05935, see similar trends in the gluon shape and improvements in  $\chi^2$

NOTE: these PDFs including low x resummation will be much more suitable for use in MC generators



# Further study of the shapes of the gluon and the sea



In fixed order fits at NNLO the gluon dips below the sea at low- $x$  as  $Q^2$  is reduced.  
 This is a general feature of NNLO fits - not just of HERAPDF.

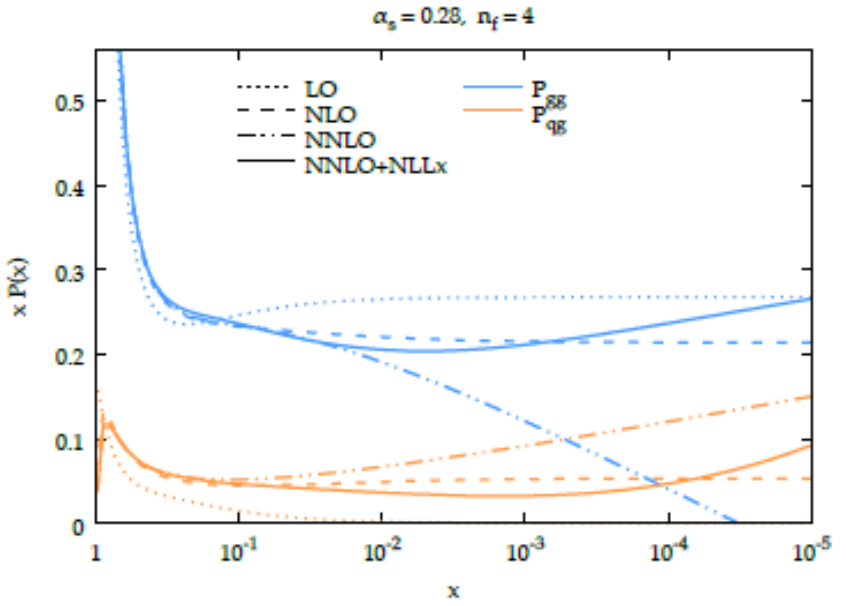
These plots show the ratio of total sea  $\Sigma$  to gluon vs  $x$  for various  $Q^2$  for NNLO and NNLO+NLLx fits.  
 The ratio is much more stable with Low  $x$  resummation

This arises from the behaviour of the  $P_{qg}$  and  $P_{gg}$  splitting functions.

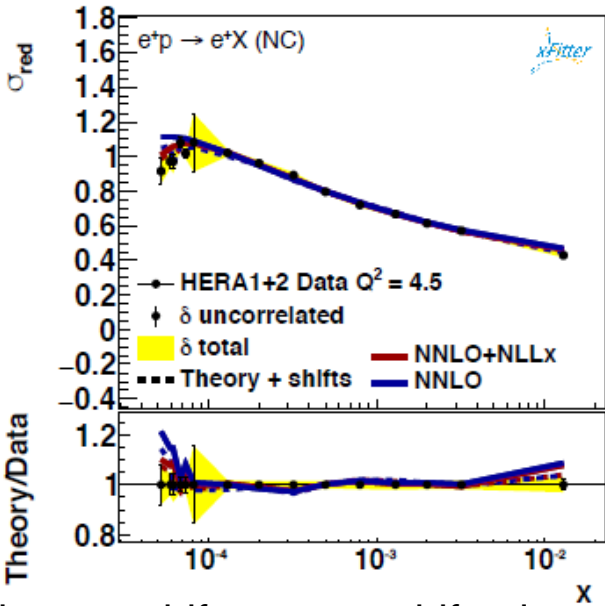
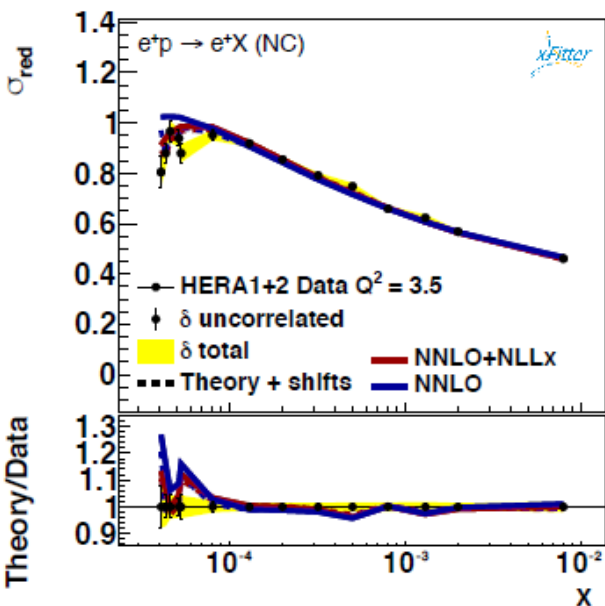
At NNLO  $xP_{qg}(x) > xP_{gg}(x)$  for  $x \lesssim 10^{-3}$ ,

Whereas for NNLO+NLLx

$$xP_{qg}(x) < xP_{gg}(x)$$



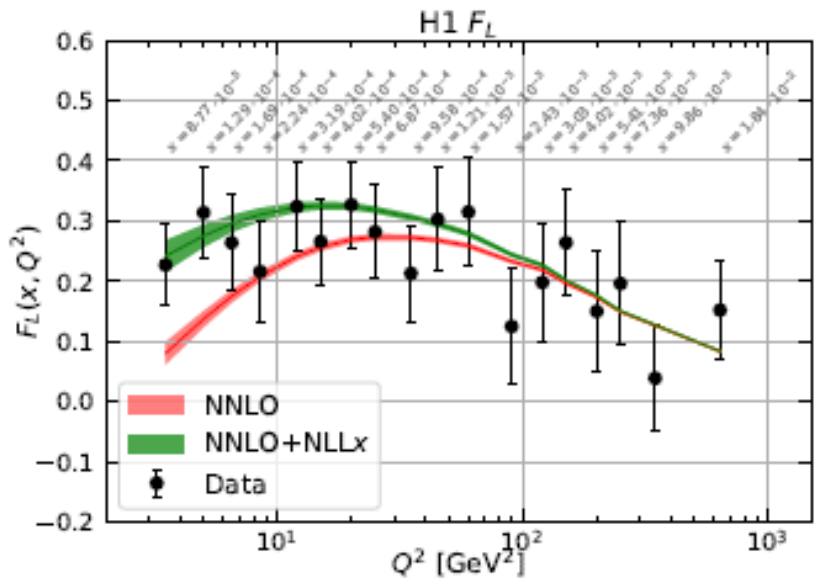
# Comparison to data



Comparison to data in the lowest  $Q^2$  bins shows that the fit with low  $x$  resummation is much better able to follow the turn over of the data that happens at low- $x$ , low  $Q^2$ , high- $y$  due to the  $F_L$  term in the reduced cross section

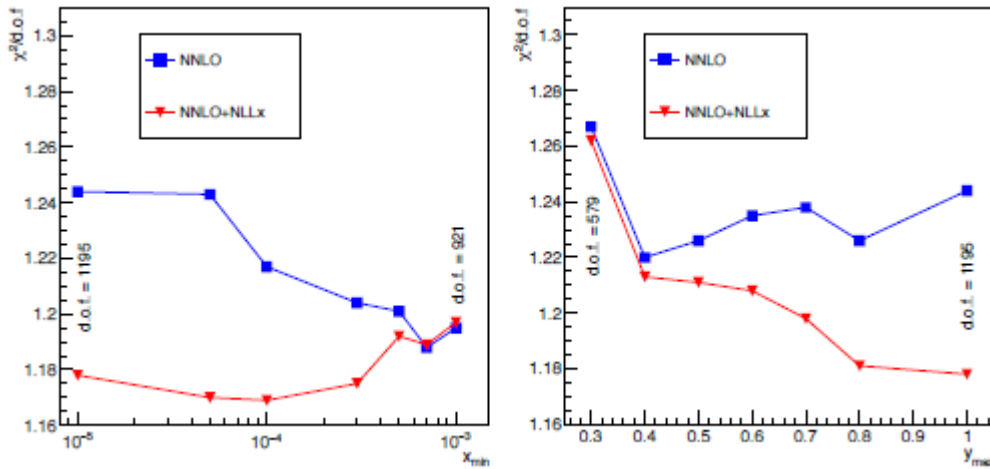
$$\sigma_{red} = F_2 - \frac{y^2}{Y_+} F_L$$

Looking at H1  $F_L$  data directly shows that  $F_L$  is larger at low  $Q^2/x$  for the NLLx fit



Theory +shifts means shifts due to experimental systematics





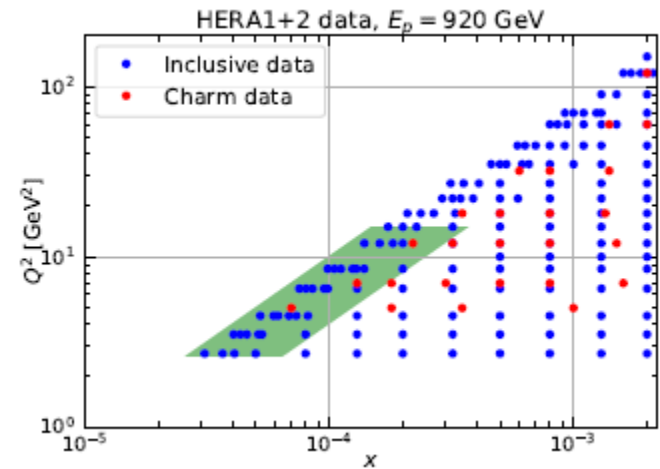
We also scan vs  $x_{min}$  seeing improvement for  $x_{min} < 5 \cdot 10^{-4}$

And against  $y_{max}$  seeing improvement for  $y_{max} > 0.4$

This emphasizes the importance of low  $x$  resummation at high- $y$  for the DIS data because of the role of the FL term

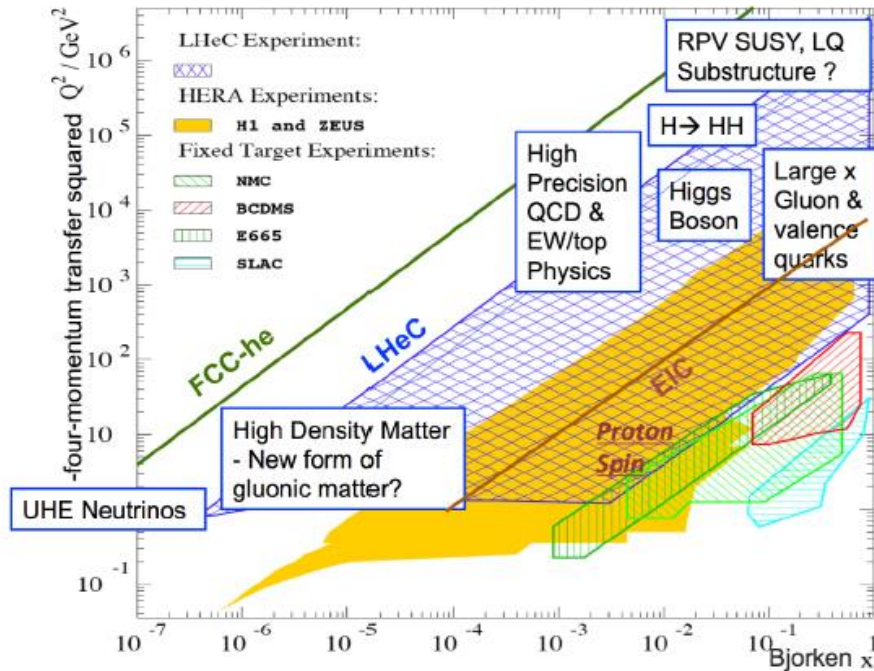
$$\sigma_{red} = F_2 - \frac{y^2}{Y_+} F_L$$

The scans shown here were done refitting the PDFs at each step—thus they delineate a region where the fixed order calculation is poor—even with refitting—as illustrated on the  $x, Q^2$  plane here.



$$H = \ln(1/x) / \ln Q^2 / \Lambda^2 \text{ with } \Lambda = 88 \text{ MeV.}$$

# LHeC and FCC-eh



**LHeC** kinematic reach:

$Q^2$  up to  $10^6 \text{ GeV}^2$

$x$  down to  $10^{-6}$

**FCC-eh** extends further,

$Q^2$  to  $10^7 \text{ GeV}^2$ ,  $x$  to  $10^{-7}$

- **outline of this talk:**
- PDFs at FCC-eh
- strong coupling ( $\alpha_s$ )

The relevance of this kinematic region to the LHeC is obvious

# Summary

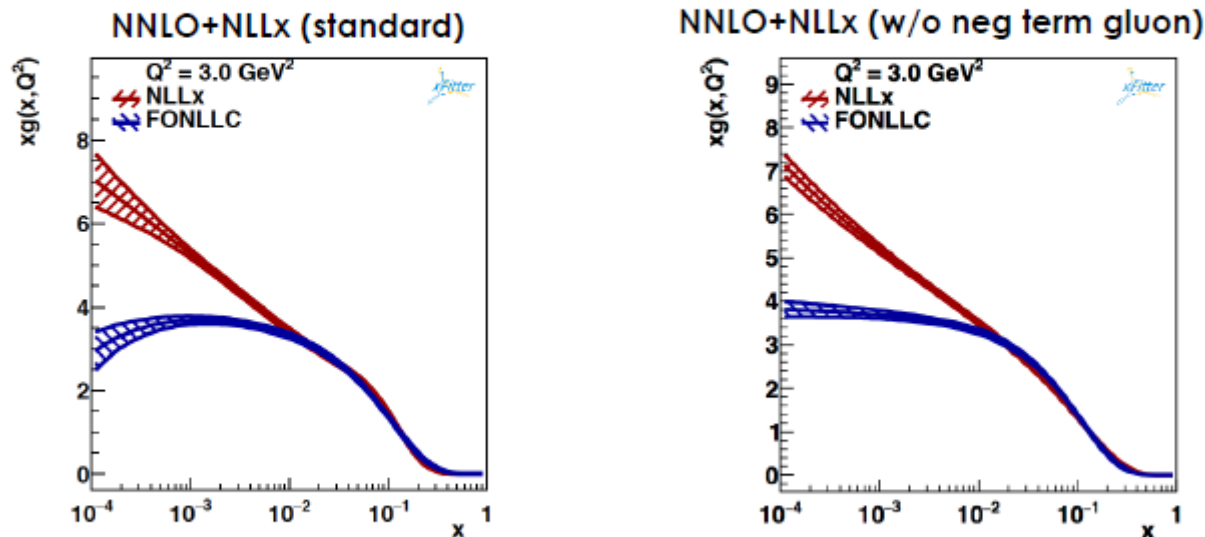
## Low-x resummation:

- Improves the description of HERA data at low-x, low- $Q^2$ , high-y, without need for further parameters (as for example when adding higher twist terms)
- Results in a rising low-x gluon, which is always larger than the total Sea

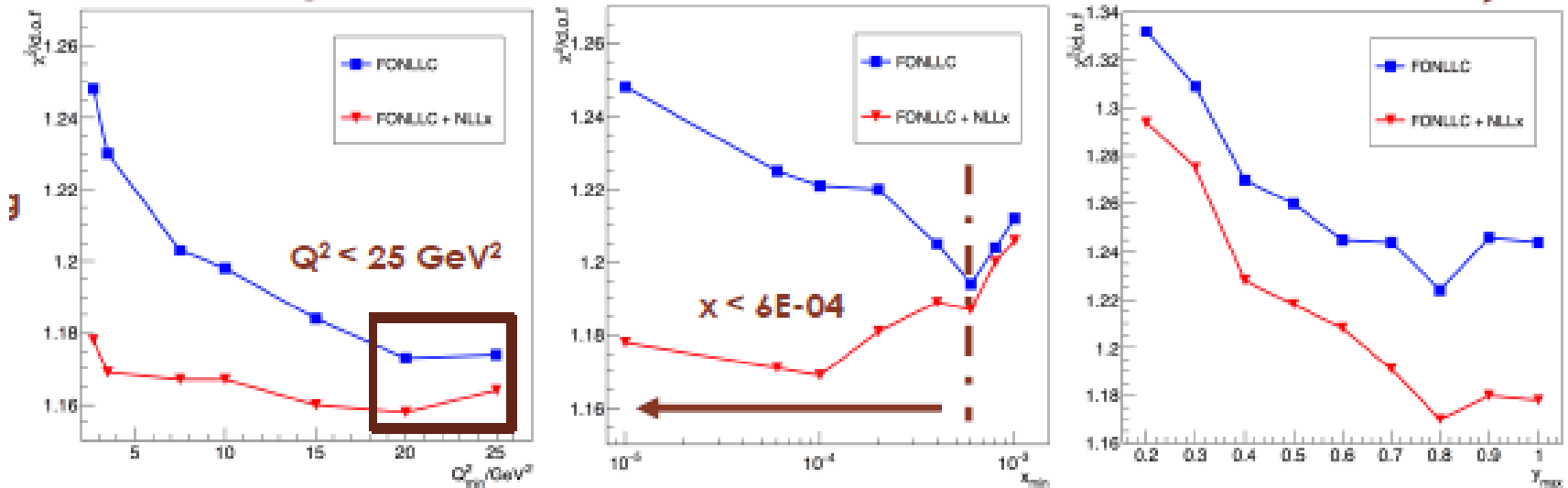
Back-up

## Adding the negative gluon term

Do we really need the negative term of gluon? → We produced a version of the **final NNLO+NLLx and NNLO fits without the negative term** just to check this



The point is that even without the negative term the gluon for NNLO likes to take a flattish shape at low- $x$ , whereas for NNLO+NLLx it takes a singular shape

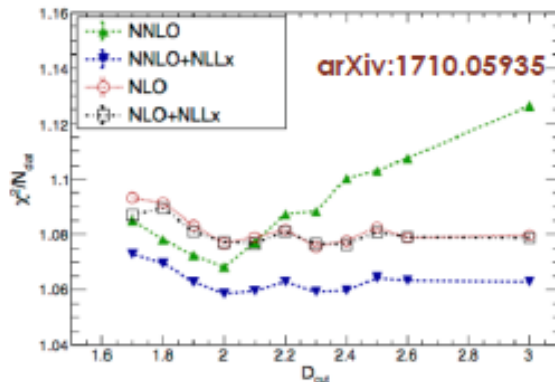
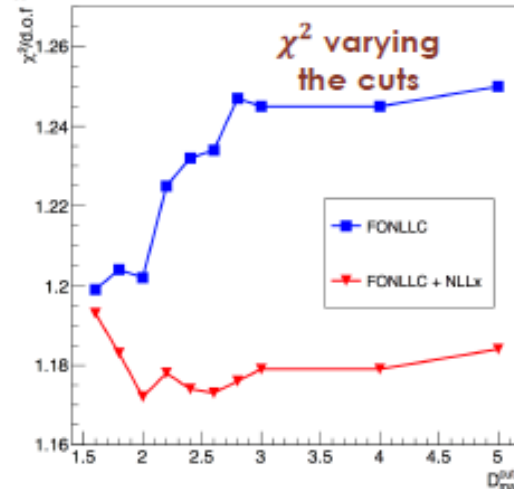
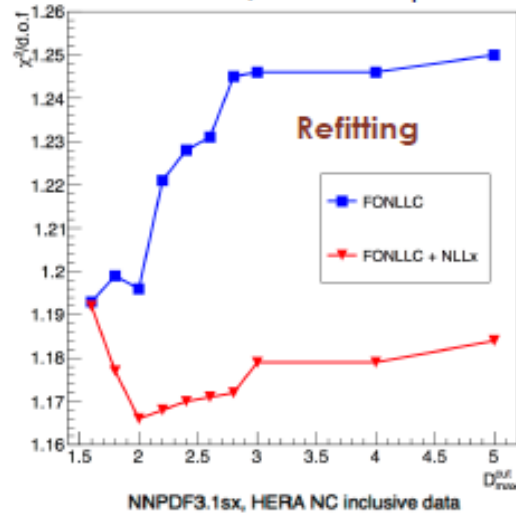


IF we do not refit at every step of the scan but we use the same PDFs as determined for the minimal cuts, we get these results.

The improvement of NLLx is still at low-x and low Q2 but is not so obviously concentrated at high-y. The refitting takes into account the need to fit DIS data for which the effect of  $F_{\text{IL}}$  is concentrated at high-y

$$\sigma_{\text{red}} = F_2 - \frac{y^2}{Y_+} F_L$$

Simultaneous cut on  $Q^2$  and  $x$  implemented:  $\ln \frac{1}{x} \geq \beta_0 H_{\text{cut}} \ln \frac{Q^2}{\Lambda^2}$   $\Lambda \simeq 88 \text{ MeV}$   $\beta_0 \simeq 0.61$



Consistent with what has been found in the NNPDF paper:

- $D_{\text{cut}} > 2$  defines the region where resummation is important
- Flat-ish  $\chi^2$  distribution for NNLO+NLLx
- Above  $D_{\text{cut}} = 3$  few data points added even if with huge steps

We could also perform a cut jointly in  $x$  and  $Q^2$  which follows the dependence of resummation terms on  $\alpha_s(Q^2) \ln(1/x)$  ie on  $\ln(1/x)/\ln(Q^2)$

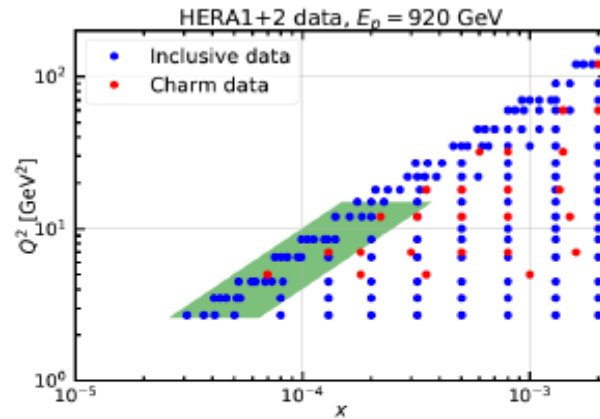


**Figure 11** Scatter plot of the low- $x$  and low- $Q^2$  kinematic region covered by the HERA1+2 inclusive data and charm data at  $E_p = 920$  GeV. The green shaded area indicates the region in which  $\ln(1/x)$  resummation has a significant effect.

Defined by:

- $x < 5 \cdot 10^{-4}$
- $2.7 \text{ GeV}^2 < Q^2 < 15 \text{ GeV}^2$
- $0.4 < y < 1.0$

Since the  $\chi^2$  scans have been obtained independently from one another, one may wonder whether our estimate is reliable.

In order to check this, we have performed two additional fits, one with and one without resummation, excluding only the data points for which  $Q^2 < 15$  GeV<sup>2</sup> and  $y > 0.4$ .

<b>--- NNLO+NLLx ---</b>			<b>--- NNLO ---</b>		
<u>After minimisation</u>	1249.201064	1.174	<u>After minimisation</u>	1264.22	1064 1.188
<u>Partial chi2s</u>			<u>Partial chi2s</u>		
395.95( +3.95)	354	HERA1+2 NCep 920	402.82( +7.25)	354	HERA1+2 NCep 920
51.32( -0.64)	56	HERA1+2 NCep 820	52.23( -0.10)	56	HERA1+2 NCep 820
179.52( -1.09)	214	HERA1+2 NCep 575	177.53( +1.15)	214	HERA1+2 NCep 575
179.12( -2.25)	170	HERA1+2 NCep 460	176.67( -0.31)	170	HERA1+2 NCep 460
222.78( -0.82)	159	HERA1+2 NCem	215.44( +1.04)	159	HERA1+2 NCem
45.59( +0.57)	39	HERA1+2 CCep	44.30( +0.35)	39	HERA1+2 CCep
53.88( -2.45)	42	HERA1+2 CCem	54.93( -1.58)	42	HERA1+2 CCem
44.53( -1.11)	44	Charm cross section	45.39( -1.31)	44	Charm cross
<u>Correlated Chi2</u> 80.329061352348674			<u>Correlated Chi2</u> 88.418716117383113		
<u>Log penalty Chi2</u> -3.8395890369565198			<u>Log penalty Chi2</u> 6.4854418695532452		

- The total  $\chi^2$ 's of these fits differ by around 15 units in favour of the resummed fit, mostly due to the correlated and logarithmic terms, to be compared to the 73 units of when the shaded area is instead included.
- This confirms that, the context of DIS, the shaded area in Fig. 11 does provide a reliable estimate of the kinematic region in which resummation works significantly better than fixed order.

